Journal of Luminescence 196 (2018) 392–398

Contents lists available at ScienceDirect

Journal of Luminescence

journal homepage: www.elsevier.com/locate/jlumin

Effectual binding of gallic acid with p-sulfonatocalix[4]arene: An experimental and theoretical interpretation

Chokalingam Saravanan[a], Ramesh Kumar Chitumalla[b], Bosco Christin Maria Arputham Ashwin[a], Marimuthu Senthilkumaran[a], Palaniswamy Suresh[c], Joonkyung Jang[b,*], Paulpandian Muthu Mareeswaran[a,*]

[a] Department of Industrial Chemistry, Alagappa University, Karaikudi, Tamilnadu, India
[b] Department of Nanoenergy Engineering, Pusan National University, Busan 609-735, Republic of Korea
[c] Department of Natural Products Chemistry, Madurai Kamaraj University, Madurai, Tamilnadu, India

ARTICLE INFO

Keywords:
p-Sulfonatocalix[4]arene
Gallic acid
Host-guest
Fluorescence
Cyclic voltammetry
NMR analysis
DFT study

ABSTRACT

The host-guest interaction of gallic acid (GA) with p-sulfonatocalix[4]arene (p-SC4) is studied using emission and excited state lifetime techniques. The quenching effect on the emission intensity and excited state lifetime is observed upon binding. The impact of oxidation potential upon binding is studied using cyclic voltammetric technique. The structural features and the mode of binding of GA with p-SC4 is examined using ^{1}H NMR and rotating frame overhauser effect spectroscopy (ROESY) techniques. The binding of GA with p-SC4 has also been examined by means of density functional theory simulations. The calculated interaction energy of GA with p-SC4 (22.15 kcal/mol) indicates the strong binding nature.

1. Introduction

The host-guest chemistry has wide range of applications from molecular recognition, drug delivery to gas storage materials. Construction of supramolecular architectures involves different types of interactions like electrostatic, hydrophobic, van der Walls, π-π, cation-π and hydrogen bonding and depends on the nature of the guest molecules [1,2]. The calixarene chemistry is a well-established field with in the supramolecular chemistry [3,4]. These phenol interlinked molecules are represented as macrocycles with enormous opportunities for synthetic tuning due to the flexible methyl bridge and functional upper and lower rims [5,6]. The plausible functionalization at the upper and lower rims can be tuned to capture selective target molecules [7]. The introduction of acid groups such as p-sulfonato-, o-phosphonato-, o-alkylcarboxylato- groups makes calixarene platforms as water soluble so as to bind with a variety of biologically interesting molecules [8–10]. p-Sulfonatocalix[4]arene (p-SC4) is an important water soluble macrocyclic compound due to its facile synthesis and appropriate cavity size [11,12]. p-SC4 possess three-dimensional, flexible, π-electron rich cavity. The additional anchoring points provided by the sulfonato groups, endows strong binding affinities and recognition properties towards several guest molecules such as metal ions, organic cations, neutral organic molecules, dyes and bio-relevant molecules [13–20]. p-SC4 has been exploited as a carrier for numerous drug molecules, which exhibit low biological toxicity, good water solubility and also to improve the solubility of water insoluble drug molecules upon supramolecular complexation [21–25].

Gallic acid (GA) (3,4,5-trihydroxybenzoic acid) is an important class of aromatic phenolic acid that can be found in great abundance in the natural sources, especially in gallnuts, citrus fruits, cereals, green tea, berries, cherries, pomegranate, grapes, honey, red wine, and herbs [26–28]. GA is also obtained from bio-synthesis of shikimate pathway by the enzyme dihydroshikimate [27]. GA and its derivatives are used in pharmaceutical, tanning, ink dye, manufacturing of paper and food industries [29,30]. GA has wide range of biochemical properties, including antioxidant, anti-inflammatory, anti-microbial, anti-carcinogenic, anti-allergic, anti-artherogenic, scavenging of free radicals, and protection against cardiovascular diseases [31–34]. Both the pro-oxidant and the anti-oxidant properties of GA facilitates cytotoxic effect against several tumor cells such as lung cancer, breast cancer, intestinal cancer, gastric cancer, prostate cancer, cervical cancer, colon cancer and skin cancer [35–40]. The electron transfer characteristics of GA is responsible for all these biological properties, therefore the electron transfer properties of GA with enzyme models such as iron and ruthenium(II) complexes have been studied previously [26,41]. The inclusion of GA with α- and β- cyclodextrin has been studied previously by

* Corresponding authors.
E-mail addresses: jkjang@pusan.ac.kr (J. Jang), mareeswaran@alagappauniversity.ac.in, muthumareeswaran@gmail.com (P. Muthu Mareeswaran).

https://doi.org/10.1016/j.jlumin.2017.12.063
Received 18 August 2017; Received in revised form 19 December 2017; Accepted 27 December 2017
Available online 28 December 2017

Rajendiran et. al.[42] In the present work, we report the inclusion of biologically important GA within p-SC4 using spectrofluorimetric, fluorescence lifetime, electrochemical and NMR techniques. To gain deeper insights into the intermolecular interaction between host and guest molecules, we performed density functional theory (DFT) simulations. The DFT calculations assist in understanding the nature and binding strength of the GA with p-SC4.

2. Experimental section

2.1. Materials

p-SC4 is synthesized by direct sulfonation of p-*tert*-butylcalix[4] arene using the literature procedure [25,43,44]. GA is procured from Avra synthesis Pvt. Ltd, Hyderabad, India. Millipore water is used as a solvent throughout the study.

2.2. Determination of binding constant from emission measurement

Fluorescence measurements are carried out using fluorescence Agilent spectrophotometer. Initially, the GA concentration is fixed at 1 $\times$ 10^{-5} M and the p-SC4 concentration is increased from 1 $\times$ 10^{-5} M to 9 $\times$ 10^{-5} M. The fluorescence intensity of GA is decreased upon addition of p-SC4. The binding constant value for this measurement is determined using modified Stern-Volmer equation [19].

$$\log[(F_0-F)/F] = n\log[H] + \log K_a \quad (1)$$

In Eq. (1), F_0 is the fluorescence intensity of GA in the absence of p-SC4, F is the fluorescence intensity of GA in the presence of p-SC4, [H] is the concentration of p-SC4, K_a is the binding constant value, n is the stoichiometric ratio of GA/p-SC4 complex. The binding ratio is determined using Job's plot method. The GA concentration is varied from 1 $\times$ 10^{-5} M to 9 $\times$ 10^{-5} M and the p-SC4 concentration is varied in the reverse order from 9 $\times$ 10^{-5} M to 1 $\times$ 10^{-5} M and the emission changes are recorded. The plot of mole fraction versus change in emission intensity gives the host-guest association for the GA with p-SC4. The quenching constant, k_q is calculated using the Stern-Volmer equation [19,45].

$$F_0/F = 1 + k_q\tau[H] \quad (2)$$

where τ is the excited state lifetime of GA.

2.3. Determination of free energy change

The free energy change, ΔG°, one of the thermodynamic functions, can be evaluated from the binding constant, K_a, values by Eq. (3).

$$\Delta G^\circ = -RT\ln K_a \quad (3)$$

In Eq. (3), ΔG° is the free energy change of the reaction, R is gas constant, T is temperature and K_a is binding constant value.

2.4. Lifetime measurement

The fluorescence lifetime of GA in the absence and in the presence of p-SC4 is recorded on HORIBA JOBIN-VYON data station using time-correlated single photon counting method (TCSPC). For this analysis, the 280 nm LED is the light source used to excite the molecule for the emission maxima of GA at 347 nm. For GA, the concentration is kept constant at 1$\times$ 10^{-4} M and the addition of varying concentration of p-SC4 is from 0.5 $\times$ 10^{-4} M to 2 $\times$ 10^{-4} M. The excited state fluorescence lifetime of GA alone and in the presence of p-SC4 were examined by plotting decay versus time using the recorded data.

2.5. Determination of binding constant from electrochemical study

The electrochemical behavior of GA and GA/p-SC4 sample solutions in aqueous medium is analyzed using cyclic voltammetry on a CHI604D electrochemical analyzer. The electrochemical cell consists of three electrode system. Glassy carbon (GC) as working electrode, silver-silver chloride as a reference electrode, and platinum as counter electrode respectively. The experiment is carried out with sample solutions without using any external electrolyte. The volume of p-SC4 is fixed at 10 ml of 10^{-3} M. The amount of GA is increased by means of incremental additions of 2 ml of 10^{-3} M of GA and vice versa. After the each 2 ml addition of host or guest, the resultant mixture was agitated for 2 min using magnetic stirrer. The binding constant value is determined using Benesi-Hildebrand equation [46,47].

$$(1/I_{HG})-I_G = 1/\Delta I + 1/K_a[GA]_0\Delta I[p-SC4]_0 \quad (4)$$

where I_G is the oxidation peak current of GA in the absence of p-SC4, I_{HG} is the oxidation peak current of the GA in the presence of p-SC4, and I_{HG} - I_G is the difference in the oxidation peak current of the GA/p-SC4 mixture and the GA alone, ΔI is the difference between the molar peak current coefficient of GA/p-SC4 complex mixture and the GA. $[GA]_0$ and $[p\text{-}SC4]_0$ are the initial concentrations of GA and p-SC4 respectively. The plot of $1/I_{HG}$ - I_G versus $1/[p\text{-}SC4]$ gives a straight line. We obtained the binding constant value from slope of the straight line. The ΔG° value is also calculated from the binding constant value K_a by using Eq. (3).

2.6. NMR technique

The binding of GA with p-SC4 is structurally investigated by NMR spectral titration using Bruker 500 MHz spectrometer. Deuterium oxide is used as solvent for ^{1}H NMR titration and for rotating frame nuclear Overhauser effect (ROESY) spectral techniques.

3. Results and discussion

The formation of stable complex of GA with p-SC4 is studied by emission, excited state lifetime, cyclic voltammetry, NMR technique and computational studies. The chemical structures of GA and p-SC4 are shown in Chart 1.

3.1. Fluorescence measurement

The emission maximum of GA is around 352 nm upon excitation at 260 nm. The emission spectrum of GA is given in Fig. S1, whereas p-SC4 does not exhibit emission properties. Therefore the emission spectroscopy can be used to study the interaction between p-SC4 and GA. The concentration of GA is fixed and the concentration of p-SC4 is varied as described in the experimental section and the emission spectra recorded. The quenching of emission intensity is observed upon increasing the concentration of p-SC4. (Fig. 1) This observation is due to the binding of GA with p-SC4. The fluorescence quenching effect on guest upon complexation with p-SC4 follows the similar trend of

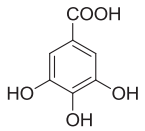

3,4,5-trihydroxybenzoic acid (or) Gallic acid (GA)

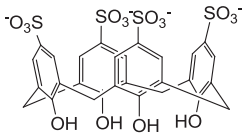

p-Sulfonatocalix[4]arene (p-SC4)

Chart 1. Structural illustration of p-sulfonatocalix[4]arene and gallic acid.

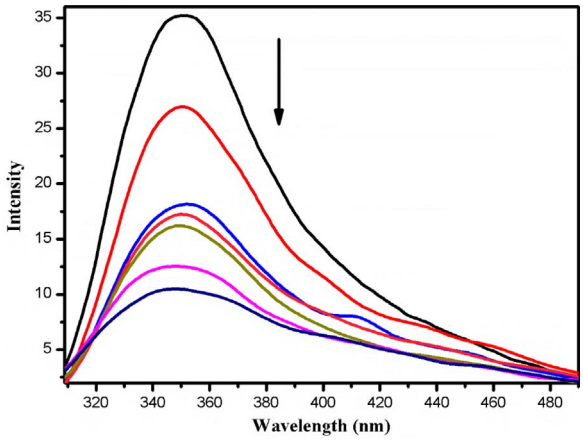

Fig. 1. The emission spectral changes of GA (1×10^{-5} M) with increasing concentration of p-SC4 (varied from 1×10^{-5} M to 9×10^{-5} M) (excited at 260 nm).

previous reports [48,49].

The binding constant value is calculated using modified Stern-Volmer equation (Eq. (1)). From the plot of log[F_0-F/F] versus log[p-SC4], the binding constant value is calculated. (Fig. S2) The calculated binding constant value is $10.2 \times 10^4\ M^{-1}$. The 1:1 binding of GA with p-SC4 is confirmed using Job's plot (Fig. 2).

The quenching constant is calculated using Stern-Volmer equation (Eq. (2)) and the value is $4.4 \times 10^{13}\ M^{-1}s^{-1}$ (Fig. S3). The high quenching constant shows the static quenching of GA with p-SC4 and the ground state complex formation. The free energy change ΔG° value calculated is -29.04 kJ mol^{-1}. The negative ΔG° value shows that the binding of GA with p-SC4 is spontaneous.

3.2. Excited state lifetime using TCSPC method

The excited state lifetime of GA, obtained from TCSPC technique, is 777.93 Ps upon excited at 280 nm. The concentration of GA is fixed at 1×10^{-4} M, the concentration of p-SC4 is varied from 0.5×10^{-4} M to 2×10^{-4} M and the excited state lifetime is recorded. The excited state lifetime of GA is decreased upon increasing the concentration of p-SC4 as shown in Fig. 3. The quenching of excited state lifetime of GA is due to the binding of GA into the p-SC4 basket.

3.3. Cyclic voltammetry technique

The cyclic voltammogram of p-SC4 is given in Fig. S4. The anodic peak of p-SC4 observed at ≈ 0.94 V is due to the oxidation of phenolic moiety of p-SC4 [50,51]. The downward potential shift of p-SC4 observed after the addition of GA, is due to the binding of p-SC4 with GA. Two anodic peaks at 0.48 V and 0.84 V, are corresponding to the formation of semiquinone radical and quinone of GA in the presence of p-SC4 [52,53]. In this case, the p-SC4 supports the GA oxidation upon

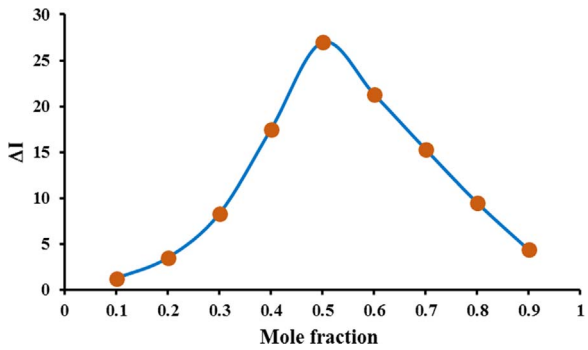

Fig. 2. Job's plot of GA with p-SC4 system from emission measurement.

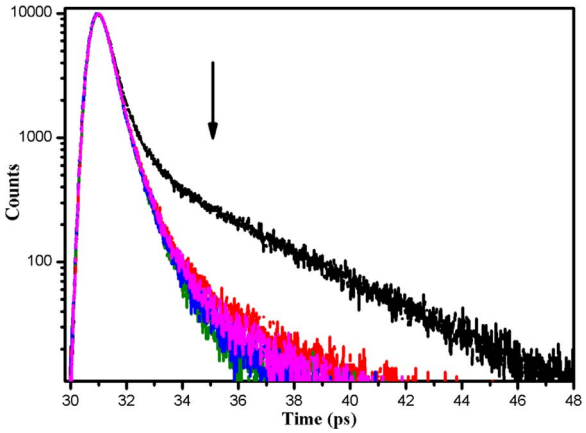

Fig. 3. The excited state lifetime changes of GA (1×10^{-4} M) with addition of varying concentration of p-SC4 (0.5×10^{-4} M to 2×10^{-4} M) (excited at 280 nm).

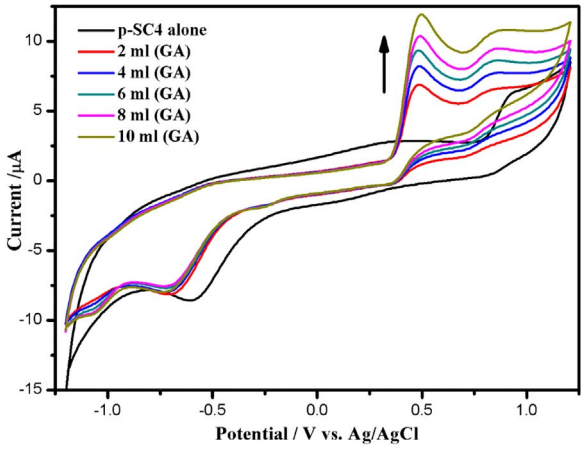

Fig. 4. Changes in the cyclic voltammogram of p-SC4 (10 ml, 10^{-3} M) on the addition of GA (2–10 ml, 10^{-3} M) (scan rate is 50 mV/s).

Table 1
Values of anodic peak potential and current of p-SC4 with change of concentration of GA.

S. No	Concentration of GA (ml, 10^{-3} M)	Epa_1 (V)	Ipa_1 (μA)	Epa_2 (V)	Ipa_2 (μA)
1	0	0.94	6.42	–	–
2	2	0.84	6.49	0.48	6.85
3	4	0.84	7.63	0.48	8.19
4	6	0.84	8.55	0.48	9.26
5	8	0.83	9.40	0.48	10.33
6	10	0.83	10.61	0.48	11.90

inclusion. Overlapping of hydroxyl oxidation of both the p-SC4 and GA is observed at 0.84 V. The enhancement in the anodic peak current observed after the addition of varying concentration of GA is shown in Fig. 4 and the changes are given in Table 1. These results show the generation of pool of protons available from the uncomplexed or free GA and the hydrogen bonding behavior also can be envisaged. The calculated binding constant value is $1.8 \times 10^3\ M^{-1}$ and the Benesi-Hildebrand plot is given in Fig. S6. The ΔG° value obtained is -18.86 KJ mol^{-1}using Eq. (3).

A shoulder like anodic peak at 0.81 V and another peak at 1.15 V correspond to the quinone formation and the polyphenol oxidation of GA [54,55] and the CV is given in Fig. S5. The oxidation current decreases upon addition of p-SC4 (Fig. 5) and the data are given in Table 2. Here also a similar downward shift in the peak potential is observed due to the binding of GA with p-SC4.

The binding constant value obtained from the change in the CV data

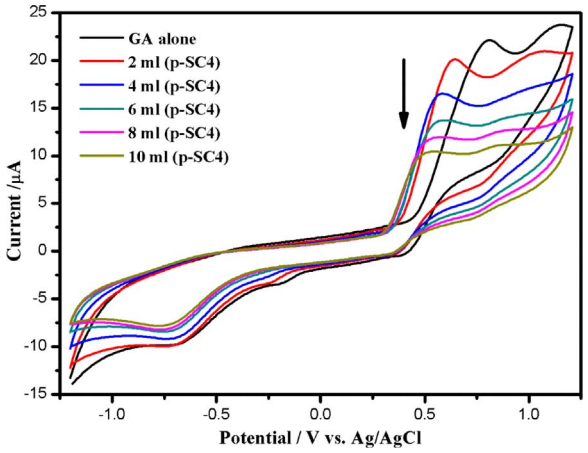

Fig. 5. Cyclic voltammogram of GA (10 ml, 10^{-3} M) with addition of p-SC4 (2–10 ml, 10^{-3} M) (scan rate is 50 mV/s).

Table 2
Anodic peak potential and current values of GA with change of concentration of p-SC4.

S. No	Concentration of p-SC4 (ml, 10^{-3} M)	Epa_1 (V)	Ipa_1 (μA)	Epa_2 (V)	Ipa_2 (μA)
1	0	0.81	22.15	1.15	23.70
2	2	0.64	20.08	1.05	20.91
3	4	0.58	16.36	0.97	16.78
4	6	0.58	13.68	0.88	13.88
5	8	0.55	11.92	0.87	12.53
6	10	0.51	10.37	0.85	11.20

is $1.8 \times 10^3\ M^{-1}$ using Eq. (4). The Benesi-Hildebrand plot for the p-SC4 on constant GA system is given in Fig. S7. The ΔG° value obtained is -18.92 KJ mol^{-1}. The decrease in current and the downward peak potential shift on the addition of p-SC4 with GA, indicate the cavity binding of GA into the p-SC4.

3.4. NMR studies

For our convenience, the protons of p-SC4 and GA are labeled as in Fig. S8. The individual ^{1}H NMR spectra of p-SC4 and GA in D_2O are shown in Figs. S9 and S10. The p-SC4 shows three characteristic peaks at 7.3, 3.75 and 1.7 ppm corresponding to the aromatic protons (Sc), −OH protons (Sb) and methylene protons (Sa) respectively. GA shows two distinct peaks at 4.7 and 7.04 ppm, which are attributed to the phenolic (-OH) protons (Ga) and the aromatic protons (Gb). The ^{1}H NMR spectral titration of GA with p-SC4 in D_2O is shown in Fig. 6. The noticeable chemical shift values are noted in GA in the presence of p-SC4 and are given in Table 3. All the –OH protons both from p-SC4 and GA are overlapped. The GA protons (Ga and Gb) show downfield shift upon introduction of p-SC4 with broadening. This is due to the interaction of GA with the upper rim of p-SC4.

The two dimensional ROESY technique is used to study the mode of binding between the GA and the p-SC4. The ROESY spectrum of GA with p-SC4 mixture (1:1) in D_2O is shown in Fig. 7.

The –OH protons (Ga) and the aromatic protons (Gb) of GA correlate with the –OH protons (Sb) and the aromatic protons (Sc) of p-SC4. There is no correlation with protons of methyl bridge of p-SC4. Therefore the binding of GA with p-SC4 is predominantly at the upper rims.

3.5. Quantum chemical calculations

We have studied the interaction of GA with p-SC4 by means of density functional theory (DFT) method. First, the optimization of

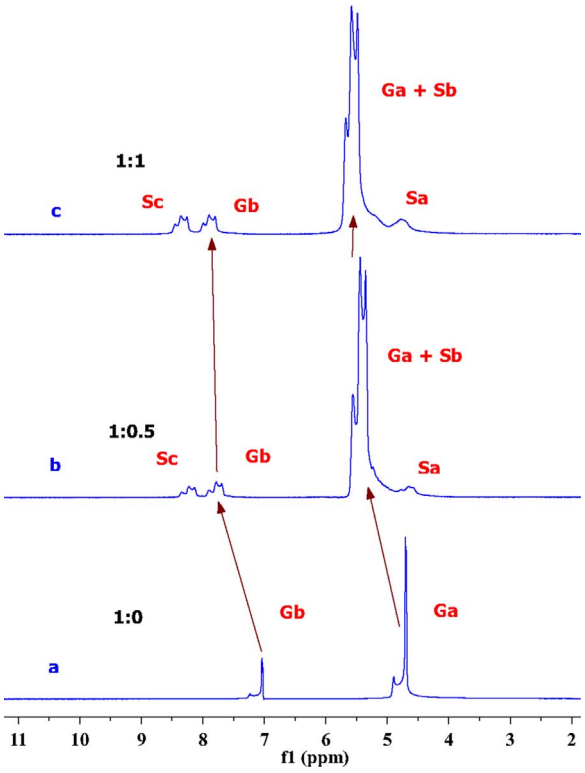

Fig. 6. ^{1}H NMR spectral titration of (a) GA alone (1:0), (b) GA with p-SC4 mixture in 1:0.5 ratio and (c) mixture of GA with p-SC4 in 1:1 ratio. The solvent peaks are omitted for clarity.

Table 3
Chemical shift values of the ^{1}H NMR spectral titration of GA with p-SC4 in D_2O.

Ratio	Ga (ppm)	Change in shift (ppm)	Gb (ppm)	Change in shift (ppm)
1:0	4.7	–	7.1	–
1:0.5	5.5	0.8	7.9	0.8
1:1	5.7	1.0	8.0	0.9

neutral GA and p-SC4 has been carried out by employing M06-2X [56] meta-hybrid exchange-correlation functional in combination with the 6-31G(d) basis set. The optimized geometries are then subjected to vibrational frequency analysis. The absence of imaginary frequencies confirms the local minima of the geometries on potential energy surface. The functional M06-2× is proven to perform very well in dealing with the H-bonding as well as non-covalent interactions. All the simulations are carried out by using Gaussian 09 quantum chemical software [57]. In the optimized geometry of p-SC4, we observed four intramolecular hydrogen bonds at the bottom of the molecule. The hydrogen atom of each -OH group is forming a hydrogen bond with the adjacent oxygen atom with a distance varying from 1.719 to 1.755 Å. The optimized geometry of p-SC4 and the four intramolecular hydrogen bonds are depicted in the Fig. 8a.

The interaction energy of GA with p-SC4 has been calculated and corrected for basis set superposition error (BSSE) using the counterpoise procedure [58]. We modeled two different possibilities for the complexation of GA with p-SC4. In the first model, the GA is oriented horizontally above the p-SC4 cavity and in the second model, the GA is placed vertically inside the cavity of p-SC4. When the GA is horizontally oriented over p-SC4, we observed four intermolecular hydrogen bonds between GA and p-SC4 (Fig. 8c). The three -OH groups of the GA are making three hydrogen bonds with 2 $-SO_3H$ groups of the p-SC4 and another hydrogen bond is formed between the -COOH of GA and $-SO_3H$

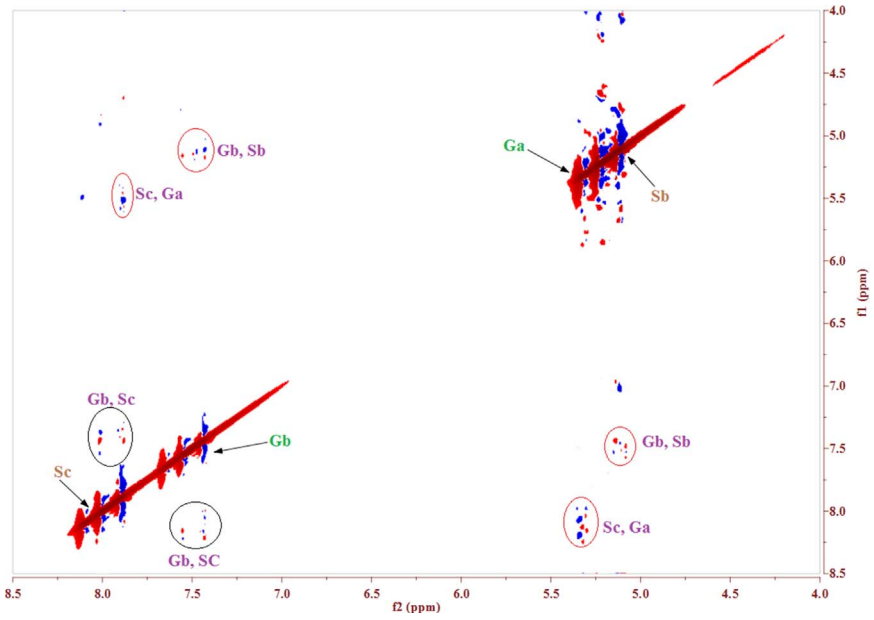

Fig. 7. ROESY spectrum of 1:1 mixture of GA with p-SC4 in D_2O.

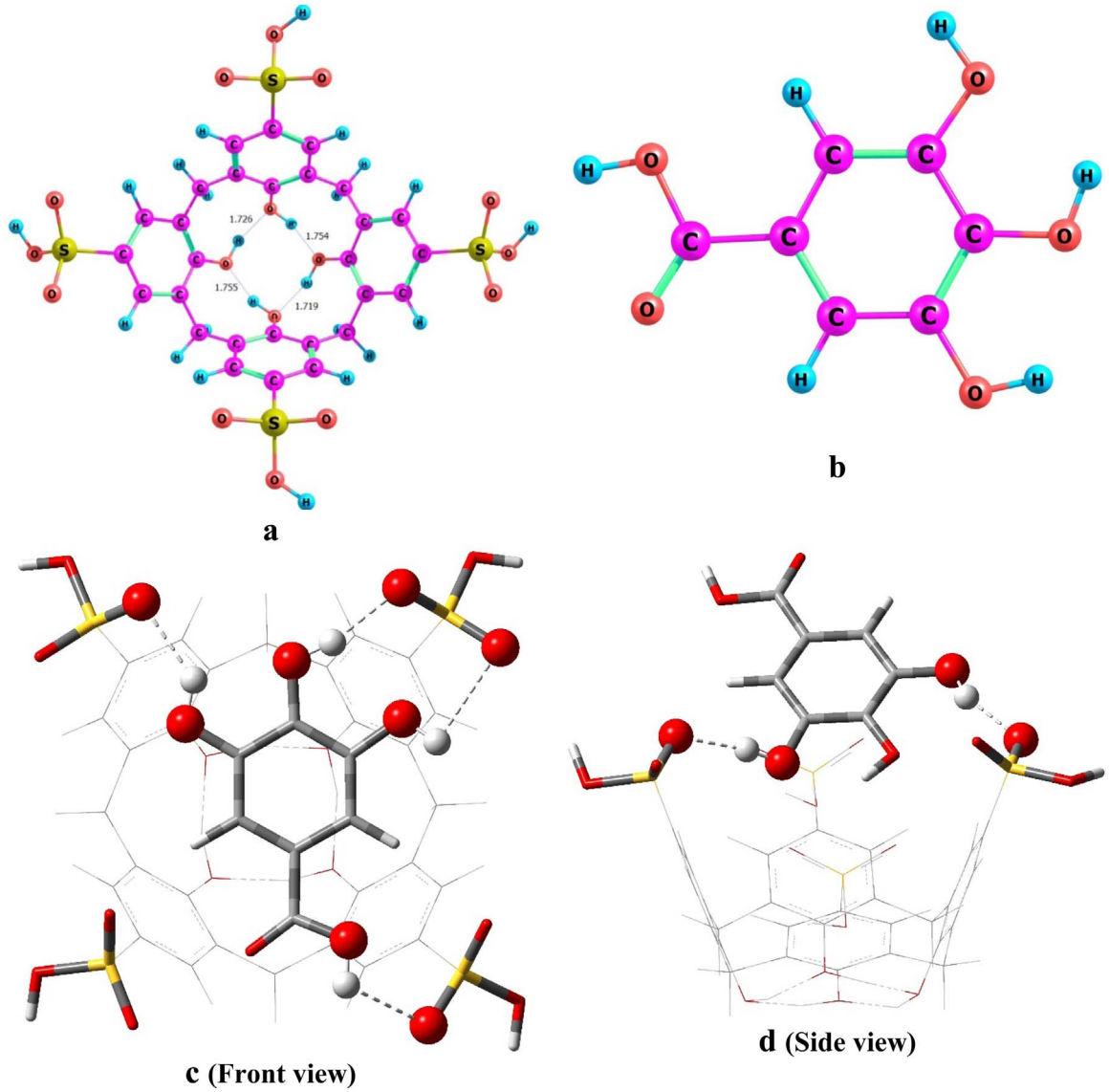

Fig. 8. The optimized geometries of (a) p-SC4, (b) GA, (c) GA (horizontal) -p-SC4, and (d) GA (vertical) -p-SC4. The hydrogen bonds are shown with dotted lines.

Table 4
Calculated interaction energies of GA with p-SC4 in horizontal and vertical orientations obtained at M06-2×/6-31G(d) level of the theory.

p-SC4-GA	BSSE uncorrected (kcal/mol)	BSSE corrected (kcal/mol)	Dipole moment (D)
Horizontal	33.48	22.15	14.49
Vertical	22.48	15.64	15.98

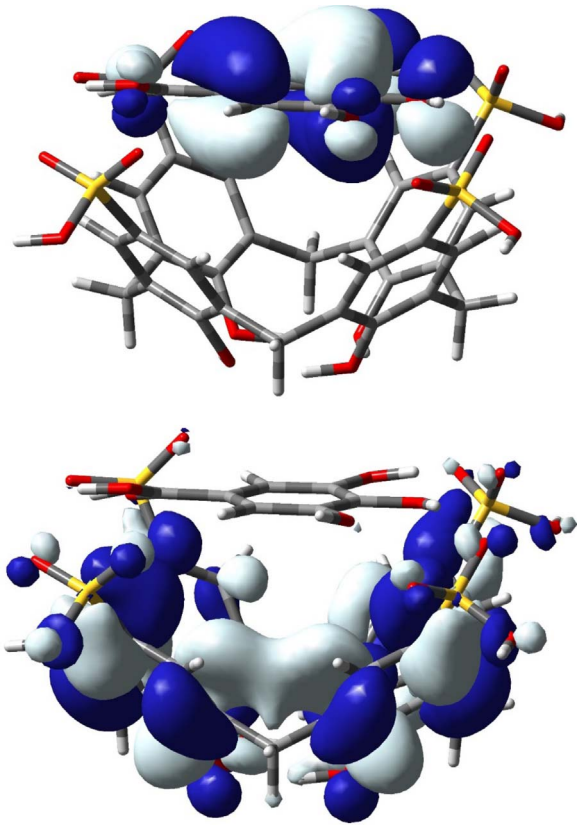

Fig. 9. HOMO (top) and LUMO (bottom) orientations of the most stable host-guest complex. Hydrogens are excluded for clarity.

of p-SC4. The hydrogen bond distances, in this case, ranged from 1.98 to 2.80 Å. The BSSE corrected interaction energy is found to be 22.15 kcal/mol for the first model. On the other hand, when the GA is oriented vertically inside the cavity of the p-SC4, we observed only two intermolecular hydrogen bonds between GA and p-SC4. These two hydrogen bonds are formed between the two -OH groups (meta positioned to -COOH) of the GA with the two -SO_3H groups of the p-SC4. In this case, the hydrogen bond distances are 1. 88 Å and 1.95 Å whereas the BSSE corrected interaction energy is 15.64 kcal/mol. The calculated interaction energies (with and without BSSE correction) and the dipole moments of the two modeled systems are given in Table 4.

The high interaction energy of the model one indicates the stable complexation between GA and p-SC4 i.e., the GA prefers to form the complex in the horizontal orientation with p-SC4. The high interaction energy of model one over model two can be attributed to the more number of intermolecular hydrogen bonds. The formation of most stable complex is chosen to investigate the charge transfer phenomenon. The electron density distribution in the frontier molecular orbitals is shown in Fig. 9.

In the HOMO, the electron density is localized towards GA and it has been completely moved to p-SC4 in LUMO, which indicates the charge transfer upon complexation.

4. Conclusion

The quenching of emission intensity of GA by p-SC4 shows efficient binding of GA with p-SC4. The static quenching of GA emission by p-SC4 confirms the ground state complex formation. Obviously the decrease in the excited state lifetime also emphasized the efficient binding. The electrochemical studies show that the downward shift in the peak potential is due to the ease of oxidation of phenol units, due to the binding of GA with p-SC4. The ^{1}H NMR spectral titration and ROESY spectral studies also confirm the stable complex formation and rim binding of p-SC4. Finally, the incorporation of GA within p-SC4 is established by theoretical simulations. Therefore the p-SC4 is the suitable as well as the most compatible host for GA.

Acknowledgements

This research was supported by Department of science and Technology (DST INSPIRE) [Project number – IFA14/CH-147], India, Korea Research Fellowship program funded by the Ministry of Science, ICT and Future Planning through the National Research Foundation of Korea (2016H1D3A1936765).

Appendix A. Supporting information

Supplementary data associated with this article can be found in the online version at doi:10.1016/j.jlumin.2017.12.063.

References

[1] V. Francisco, N. Basílio, L. García-Río, Ionic exchange in p-Sulfonatocalix[4]arene-mediated formation of metal–ligand complexes, J. Phys. Chem. B 118 (2014) 4710–4716.
[2] G. Zheng, W. Fan, S. Song, H. Guo, H. Zhang, Guests inducing p-sulfonatocalix[4]arenes into nanocapsule and layer structure, J. Solid State Chem. 183 (2010) 1457–1463.
[3] M.K. Abd El-Rahman, A.M. Mahmoud, A novel approach for spectrophotometric determination of succinylcholine in pharmaceutical formulation via host-guest complexation with water-soluble p-sulfonatocalixarene, RSC Adv. 5 (2015) 62469–62476.
[4] B. Mokhtari, K. Pourabdollah, Applications of calixarene nano-baskets in pharmacology, J. Incl. Phenom. Macrocycl. Chem. 73 (2012) 1–15.
[5] K. Kurzątkowska, S. Sayin, M. Yilmaz, H. Radecka, J. Radecki, Calix[4]arene derivatives as dopamine hosts in electrochemical sensors, Sens. Actuators B 218 (2015) 111–121.
[6] Q. Li, D.-S. Guo, H. Qian, Y. Liu, Complexation of p-sulfonatocalixarenes with local anaesthetics guests: binding structures, stabilities, and thermodynamic origins, Eur. J. Org. Chem. 2012 (2012) 3962–3971.
[7] J. Chao, Z. Li, Y. Liu, Y. Zhang, Z. Guo, B. Zhang, X. Wang, Investigation of the inclusion interaction of p-sulfonatocalix[6]arene with trimebutine maleate, J. Mol. Liq. 213 (2016) 173–178.
[8] O. Danylyuk, B. Leśniewska, K. Suwinska, N. Matoussi, A.W. Coleman, Structural diversity in the crystalline complexes of para-sulfonato-calix[4]arene with bipyridinium derivatives, Cryst. Growth Des. 10 (2010) 4542–4549.
[9] G. Arena, A. Casnati, A. Contino, A. Magri, F. Sansone, D. Sciotto, R. Ungaro, Inclusion of naturally occurring amino acids in water soluble calix[4]arenes: a microcalorimetric and ^{1}H NMR investigation supported by molecular modeling, Org. Biomol. Chem. 4 (2006) 243–249.
[10] F. Perret, A.N. Lazar, A.W. Coleman, Biochemistry of the para-sulfonato-calix[n]arenes, Chem. Commun. (2006) 2425–2438.
[11] P.M. Gharat, S. Joseph, M. Sundararajan, S. Dutta Choudhury, H. Pal, Contrasting tunability of quinizarin fluorescence with p-sulfonatocalix[4,6]arene hosts, Org. Biomol. Chem. (2016).
[12] Z. Qin, D.-S. Guo, X.-N. Gao, Y. Liu, Supra-amphiphilic aggregates formed by p-sulfonatocalix[4]arenes and the antipsychotic drug chlorpromazine, Soft Matter 10 (2014) 2253–2263.
[13] B.C.M.A. Ashwin, R.K. Chitumalla, A. Herculin Arun Baby, J. Jang, P. Muthu Mareeswaran, Spectral, electrochemical and computational investigations on the host–guest interaction of Coumarin-460 with p-sulfonatocalix[4]arene, J. Incl. Phenom. Macrocycl. Chem. (2017), http://dx.doi.org/10.1007/s10847-017-0762-0.
[14] B.C.M.A. Ashwin, A. Herculin Arun Baby, M. Prakash, M. Hochlaf, P. Muthu Mareeswaran, A combined experimental and theoretical study on p-sulfonatocalix[4]arene encapsulated 7-methoxycoumarin, J. Phys. Org. Chem. (2017), http://dx.doi.org/10.1002/poc.3788.
[15] M. Senthilkumaran, K. Maruthanayagam, G. Vigneshkumar, R.K. Chitumalla, J. Jang, P. Muthu Mareeswaran, Spectral, electrochemical and computational investigations of binding of n-(4-hydroxyphenyl)-imidazole with p-sulfonatocalix[4]

arene, J. Fluoresc. 27 (2017) 2159–2168.
[16] G.-F. Wang, X.-L. Ren, M. Zhao, X.-L. Qiu, A.-D. Qi, Paraquat detoxification with p-sulfonatocalix-[4]arene by a pharmacokinetic study, J. Agric. Food Chem. 59 (2011) 4294–4299.
[17] B.C.M.A. Ashwin, A. Vinothini, T. Stalin, P. Muthu Mareeswaran, Synthesis of a Safranin T - p-sulfonatocalix[4]arene complex by means of supramolecular complexation, ChemistrySelect 2 (2017) 931–936.
[18] K. Madasamy, S. Gopi, M.S. Kumaran, S. Radhakrishnan, D. Velayutham, P.M. Mareeswaran, M. Kathiresan, A supramolecular investigation on the interactions between ethyl terminated bis–viologen derivatives with sulfonato calix[4]arenes, ChemistrySelect 2 (2017) 1175–1182.
[19] P. Muthu Mareeswaran, M. Prakash, V. Subramanian, S. Rajagopal, Recognition of aromatic amino acids and proteins with p-sulfonatocalix[4]arene – a luminescence and theoretical approach, J. Phys. Org. Chem. 25 (2012) 1217–1227.
[20] C. Saravanan, M. Senthilkumaran, B.C.M.A. Ashwin, P. Suresh, P. Muthu Mareeswaran, Spectral and electrochemical investigation of 1,8-diaminonaphthalene upon encapsulation of p-sulfonatocalix[4]arene, J. Incl. Phenom. Macrocycl. Chem. 88 (2017) 239–246.
[21] Y. Wenzhan, P.O. Daniel, L. Wilna, Md.V. Melgardt, Effect of para-sulfonato-calix [n]arenes on the solubility, chemical stability, and bioavailability of a water insoluble drug nifedipine, Curr. Drug Discov. Technol. 5 (2008) 129–139.
[22] W. Yang, M.M. de Villiers, The solubilization of the poorly water soluble drug nifedipine by water soluble 4-sulphonic calix[n]arenes, Eur. J. Pharm. Biopharm. 58 (2004) 629–636.
[23] W. Yang, M.M. de Villiers, Aqueous solubilization of furosemide by supramolecular complexation with 4-sulphonic calix[n]arenes, J. Pharm. Pharmacol. 56 (2004) 703–708.
[24] J. Song, H. Li, J. Chao, C. Dong, S. Shuang, Spectroscopic studies on the inclusion interaction of p-sulfonatocalix[6]arene with vitamin B6, J. Incl. Phenom. Macrocycl. Chem. 72 (2012) 389–395.
[25] P. Muthu Mareeswaran, E. Babu, V. Sathish, B. Kim, S.I. Woo, S. Rajagopal, p-Sulfonatocalix[4]arene as a carrier for curcumin, New J. Chem. 38 (2014) 1336–1345.
[26] A.E. Fazary, M. Taha, Y.-H. Ju, Iron complexation studies of gallic acid, J. Chem. Eng. Data 54 (2009) 35–42.
[27] C.G. da Rosa, C.D. Borges, R.C. Zambiazi, M.R. Nunes, E.V. Benvenutti, S.Rd Luz, R.F. D'Avila, J.K. Rutz, Microencapsulation of gallic acid in chitosan, β-cyclodextrin and xanthan, Ind. Crops Prod. 46 (2013) 138–146.
[28] T. Marino, A. Galano, N. Russo, Radical scavenging ability of gallic acid toward OH and OOH radicals. Reaction mechanism and rate constants from the density functional theory, J. Phys. Chem. B 118 (2014) 10380–10389.
[29] S. Shojaei, N. Nasirizadeh, M. Entezam, M. Koosha, M. Azimzadeh, An electrochemical nanosensor based on molecularly imprinted polymer (MIP) for detection of gallic acid in fruit juices, Food Anal. Methods 9 (2016) 2721–2731.
[30] Y. Deligiannakis, G.A. Sotiriou, S.E. Pratsinis, Antioxidant and antiradical SiO_2 nanoparticles covalently functionalized with gallic acid, ACS Appl. Mater. Interfaces 4 (2012) 6609–6617.
[31] R. Abdel-Hamid, E.F. Newair, Adsorptive stripping voltammetric determination of gallic acid using an electrochemical sensor based on polyepinephrine/glassy carbon electrode and its determination in black tea sample, J. Electroanal. Chem. 704 (2013) 32–37.
[32] F. Gao, D. Zheng, H. Tanaka, F. Zhan, X. Yuan, F. Gao, Q. Wang, An electrochemical sensor for gallic acid based on Fe_2O_3/electro-reduced graphene oxide composite: estimation for the antioxidant capacity index of wines, Mater. Sci. Eng. C 57 (2015) 279–287.
[33] H.-L. Huang, C.-C. Lin, K.-C.G. Jeng, P.-W. Yao, L.-T. Chuang, S.-L. Kuo, C.-W. Hou, Fresh green tea and gallic acid ameliorate oxidative stress in kainic acid-induced status epilepticus, J. Agric. Food Chem. 60 (2012) 2328–2336.
[34] J.-Y. Lai, L.-J. Luo, Antioxidant gallic acid-functionalized biodegradable in situ gelling copolymers for cytoprotective antiglaucoma drug delivery systems, Biomacromolecules 16 (2015) 2950–2963.
[35] C. Liu, J.-J. Lin, Z.-Y. Yang, C.-C. Tsai, J.-L. Hsu, Y.-J. Wu, Proteomic study reveals a co-occurrence of gallic acid-induced apoptosis and glycolysis in B16F10 melanoma cells, J. Agric. Food Chem. 62 (2014) 11672–11680.
[36] D.K. Maurya, N. Nandakumar, T.P.A. Devasagayam, Anticancer property of gallic acid in A549, a human lung adenocarcinoma cell line, and possible mechanisms, J. Clin. Biochem. Nutr. 48 (2011) 85–90.
[37] J.-D. Hsu, S.-H. Kao, T.-T. Ou, Y.-J. Chen, Y.-J. Li, C.-J. Wang, Gallic acid induces G2/M phase arrest of breast cancer cell MCF-7 through stabilization of p27Kip1 attributed to disruption of p27Kip1/Skp2 complex, J. Agric. Food Chem. 59 (2011) 1996–2003.
[38] M. Kaur, B. Velmurugan, S. Rajamanickam, R. Agarwal, C. Agarwal, Gallic acid, an active constituent of grape seed extract, exhibits anti-proliferative, pro-apoptotic and anti-tumorigenic effects against prostate carcinoma xenograft growth in nude mice, Pharm. Res. 26 (2009) 2133–2140.
[39] B.R. You, W.H. Park, The effects of mitogen-activated protein kinase inhibitors or small interfering RNAs on gallic acid-induced HeLa cell death in relation to reactive oxygen species and glutathione, J. Agric. Food Chem. 59 (2011) 763–771.
[40] J.A. Jara, V. Castro-Castillo, J. Saavedra-Olavarría, L. Peredo, M. Pavanni, F. Jaña, M.E. Letelier, E. Parra, M.I. Becker, A. Morello, U. Kemmerling, J.D. Maya, J. Ferreira, Antiproliferative and uncoupling effects of delocalized, lipophilic, cationic gallic acid derivatives on cancer cell Lines. Validation in vivo in singenic mice, J. Med. Chem. 57 (2014) 2440–2454.
[41] A. Rajeswari, A. Ramdass, P. Muthu Mareeswaran, S. Rajagopal, Electron transfer studies of ruthenium(II) complexes with biologically important phenolic acids and tyrosine, J. Fluoresc. 26 (2016) 531–543.
[42] R.K. Sankaranarayanan, S. Siva, A. Antony Muthu Prabhu, N. Rajendiran, A study on the inclusion complexation of 3,4,5-trihydroxybenzoic acid with β-cyclodextrin at different pH, J. Incl. Phenom. Macrocycl. Chem. 67 (2010) 461–470.
[43] D. Xiong, M. Chen, H. Li, Synthesis of para-sulfonatocalix[4]arene-modified silver nanoparticles as colorimetric histidine probes, Chem. Commun. (2008) 880–882.
[44] D.M. Miller-Shakesby, B.P. Burke, S. Nigam, G.J. Stasiuk, T.J. Prior, S.J. Archibald, C. Redshaw, Synthesis, structures and cytotoxicity studies of p-sulfonatocalix[4]arene lanthanide complexes, Cryst. Eng. Comm. 18 (2016) 4977–4987.
[45] J.R. Lakowicz, Principles of Fluorescence Spectroscopy, Springer, US, 2007.
[46] K. Srinivasan, K. Kayalvizhi, K. Sivakumar, T. Stalin, Study of inclusion complex of β-cyclodextrin and diphenylamine: photophysical and electrochemical behaviors, Spectrochim. Acta A: Mol. Biomol. Spectrosc. 79 (2011) 169–178.
[47] K. Paramasivaganesh, K. Srinivasan, A. Manivel, S. Anandan, K. Sivakumar, S. Radhakrishnan, T. Stalin, Studies on inclusion complexation between 4,4′-dihydroxybiphenyl and β-cyclodextrin by experimental and theoretical approach, J. Mol. Struct. 1048 (2013) 399–409.
[48] S.M. Mc Dermott, D.A. Rooney, C.B. Breslin, Complexation study and spectrofluorometric determination of the binding constant for diquat and p-sulfonatocalix [4]arene, Tetrahedron 68 (2012) 3815–3821.
[49] B.C.M.A. Ashwin, C. Saravanan, M. Senthilkumaran, R. Sumathi, P. Suresh, P. Muthu Mareeswaran, Spectral and electrochemical investigation of p-sulfonatocalix[4]arene-stabilized vitamin E aggregation, Supramol. Chem. 30 (2018) 32–41, http://dx.doi.org/10.1080/10610278.2017.1351612.
[50] G. Diao, W. Zhou, The electrochemical behavior of p-sulfonated calix[4]arene, J. Electroanal. Chem. 567 (2004) 325–330.
[51] G. Diao, Y. Liu, The electrochemical behavior of p-sulfonated sodium salt of calix[6]arene, Electroanalysis 17 (2005) 1279–1284.
[52] J.H. Luo, B.L. Li, N.B. Li, H.Q. Luo, Sensitive detection of gallic acid based on polyethyleneimine-functionalized graphene modified glassy carbon electrode, Sens. Actuators B 186 (2013) 84–89.
[53] M. Díaz González, T. Vidal, T. Tzanov, Electrochemical study of phenolic compounds as enhancers in laccase-catalyzed oxidative reactions, Electroanalysis 21 (2009) 2249–2257.
[54] R. Abdel-Hamid, E.F. Newair, Electrochemical behavior of antioxidants: I. Mechanistic study on electrochemical oxidation of gallic acid in aqueous solutions at glassy-carbon electrode, J. Electroanal. Chem. 657 (2011) 107–112.
[55] M. Panizza, G. Cerisola, Electrochemical degradation of gallic acid on a BDD anode, Chemosphere 77 (2009) 1060–1064.
[56] Y. Zhao, D. Truhlar, The M06 suite of density functionals for main group thermochemistry, thermochemical kinetics, noncovalent interactions, excited states, and transition elements: two new functionals and systematic testing of four M06-class functionals and 12 other functionals, Theor. Chem. Acc. 120 (2008) 215–241.
[57] M.J. Frisch, G.W. Trucks, H.B. Schlegel, G.E. Scuseria, M.A. Robb, J.R. Cheeseman, G. Scalmani, V. Barone, B. Mennucci, G.A. Petersson, H. Nakatsuji, M. Caricato, X. Li, H.P. Hratchian, A.F. Izmaylov, J. Bloino, G. Zheng, J.L. Sonnenberg, M. Hada, M. Ehara, K. Toyota, R. Fukuda, J. Hasegawa, M. Ishida, T. Nakajima, Y. Honda, O. Kitao, H. Nakai, T. Vreven, J.A. Montgomery, J.E. Peralta, F. Ogliaro, M. Bearpark, J.J. Heyd, E. Brothers, K.N. Kudin, V.N. Staroverov, R. Kobayashi, J. Normand, K. Raghavachari, A. Rendell, J.C. Burant, S.S. Iyengar, J. Tomasi, M. Cossi, N. Rega, J. M. Millam, M. Klene, J.E. Knox, J.B. Cross, V. Bakken, C. Adamo, J. Jaramillo, R. Gomperts, R.E. Stratmann, O. Yazyev, A.J. Austin, R. Cammi, C. Pomelli, J.W. Ochterski, R.L. Martin, K. Morokuma, V.G. Zakrzewski, G.A. Voth, P. Salvador, J.J. Dannenberg, S. Dapprich, A.D. Daniels, Farkas, J.B. Foresman, J.V. Ortiz, J. Cioslowski, D.J. Fox, Gaussian 09, Revision B.01, in, Wallingford CT, 2009.
[58] S.F. Boys, F. Bernardi, The calculation of small molecular interactions by the differences of separate total energies. Some procedures with reduced errors, Mol. Phys. 19 (1970) 553–566.